euronoise

An integrated multimodal acoustic particle manipulator and optical waveguide sensor

Peter Glynne-Jones[a], Fan Zhang[b], Liqin Dong[a], Rosemary Townsend[a], Nicholas Harris[c], Tracy Melvin[b], James Wilkinson[b] and Martyn Hill[a]

[a]University of Southampton, School of Engineering Sciences, University Road, SO17 1BJ Southampton, UK
[b]University of Southampton, Optoelectronics Research Centre, SO17 1BJ Southampton, UK
[c]University of Southampton, Electronics and Computer Science, SO17 1BJ Southampton, UK
p.glynne-jones@soton.ac.uk

An acoustic/optical/microfluidic system is presented for the manipulation of bead-tagged DNA and other bio-molecules. Acoustic radiation forces are used to manipulate microspheres into and away from the evanescent field of a laser coupled waveguide that is integrated into the reflector of the acoustic chamber. With suitable fluorophores the presence of the target bio-molecules can be detected with a fluorescence microscope enabling large populations of beads to be examined simultaneously.

The integrated waveguide and multi-modal acoustic chamber is presented here, with results showing that the microspheres can be successfully detected as they are brought into the evanescent field using a quarter-wave acoustic configuration. It is also shown that by measuring the time of flight of a microsphere between the half and quarter-wave nodal planes the bead size can be determined, providing a means of multiplexing the detection.

1 Introduction

Microbead assays have many advantages over planar, plate-based assays. For immuno-assays, the need to renew sensing surfaces, made difficult by the strong affinity between antigen-antibody interactions, can be overcome by flowing disposable functionalised microbeads into a microfluidic sensor. This has conventionally been accomplished by using magnetic microbeads that can be immobilised with a magnet within a sensor [1, 2]. Other assays utilising the hybridization of complementary DNA probes show a potential for great flexibility of target analytes [3], especially when combined with recent advances in multiplexed optical coding of microbeads using quantum dots [4]. Microbead assays also offer fast response times due to their high surface area, and a lower cost.

Using acoustic radiation forces to manipulate microbeads within sensor structures has the potential to offer a more flexible and controllable means of localising and trapping microbeads than magnetic techniques. A variety of approaches to manipulation have been reported, including the use of focussed ultrasound [5] or near-field effects [6] to trap particles, the use of two or more transducers to modulate the standing wave field [7], or the use of plate waves coupled into the containing fluid to excite the field [8]. However, the use of a planar layered resonator with a single transducer [9-11] offers a simple approach to establishing a USW suitable for particle movement.

Fluorescence-based planar waveguide sensing technology using a surface-confined evanescent field is widely used in biosensors and chemical sensors in order to achieve lower detection limits, reduced sample consumption and an increased degree of multiplexing capability[12]. An optical evanescent field is produced when light is guided along a waveguide, undergoing total internal reflection at an interface. The field decays exponentially with the distance from the interface or the waveguide surface; the penetration depth — the distance from the surface at which the field is 1/e of its original value at the surface — is a function of the refractive indices and dimensions of the waveguide and the medium, and is generally of the order of 100nm. An advantage of using this type of illumination to view beads near a waveguide is that light only reaches those beads manipulated to the waveguide surface.

The device presented in this paper consists of a multi-modal ultrasonic-standing-wave particle manipulator with an optical waveguide integrated into its glass (acoustic) reflector layer. By coupling laser light into the waveguide, the resulting evanescent field illuminates microbeads when they are moved onto the surface of the waveguide. A CCD camera or fluorescence microscope can be used to detect the microbeads. This paper demonstrates the device, and shows how it can be used to distinguish between beads of different sizes in a mixture, opening the possibility of using it in future work to assist in multiplexing between beads of different sizes.

2 Acoustic Design

Figure 1 shows the design of the device, and Table 1 lists its key dimensions. It comprises a circular PZT transducer (Ferroperm, PZT26) with silver electrodes glued (Epotek 301 epoxy) to a carrier layer milled from Macor (a machinable ceramic material). A steel spacer fixes the height of the chamber, which is bounded by a moulded silicone elastomer gasket. The chamber is disc shaped, with two 1mm wide channels leading to inlet ports in the carrier layer. These ports connect to a PMMA manifold, permitting fluidic connectors to deliver a bead / water mixture to the chamber under the action of a peristaltic pump. The reflector layer (all references to *reflector* in this paper will refer to this acoustic reflector, and not to any optical device) is formed from a rectangular BK7 glass slide – this incorporates an optical waveguide (see below). The ultrasonic transducer is driven by an RF-amplifier (ENI 240L) with a sinewave generated by a signal generator (TTi TG1304).

The acoustic properties of the chamber were designed using a one dimensional transfer impedance model [11], which treats the device as an ideal planar structure with plane waves travelling only in the thickness direction. This simplification ignores any lateral acoustic modes, but is sufficiently accurate to design for several different axial modes within a single device. The transducer representation described in [11] was replaced by a KLM circuit model [13] extending the operating frequency of the model beyond the first resonance. The precise frequencies and amplitudes of the resulting modes will be influenced by lateral acoustic modes, but examination of the modelled results gives good insight into operation of the device.

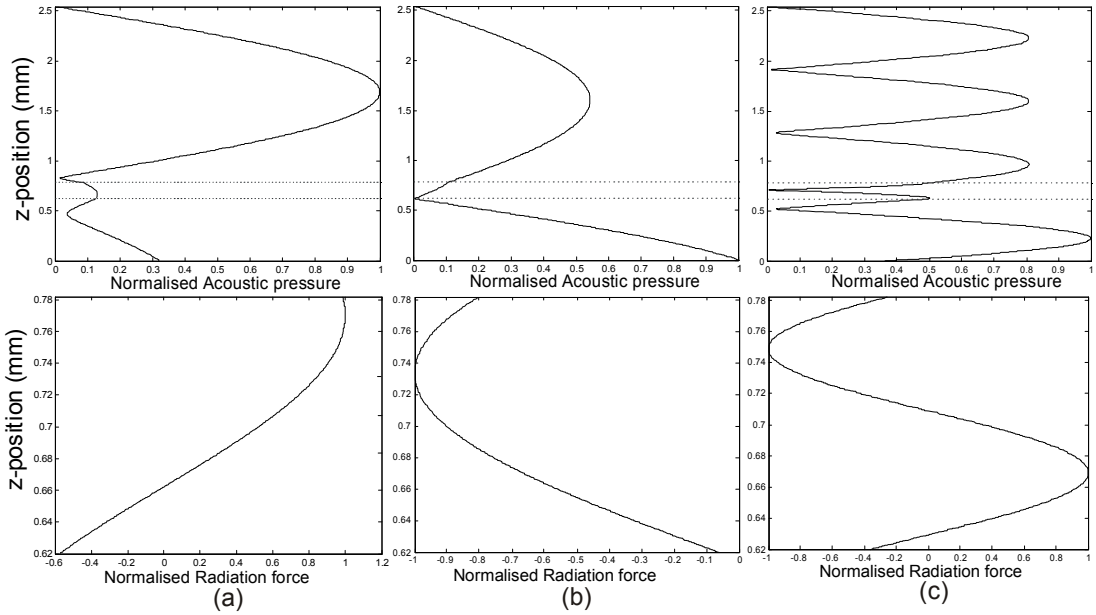

Figure 2: Device mode acoustic pressure amplitude and fluid layer radiation force profiles (modelled) for:

(a) reflector-quarter wave,
(b) carrier-quarter wave, and
(c) half-wave modes.

Dotted lines indicate the position of the fluid layer. The y-axis label 'position' refers to the distance from transducer/carrier-layer boundary. A positive force corresponds to a force towards the reflector.

Parameter	*Circular Chamber*
Transducer thickness	1.00
Carrier layer thickness	0.650
Fluid layer thickness	0.162
Reflector thickness	1.762
Transducer diameter	10

Table 1: Key device parameters (mm)

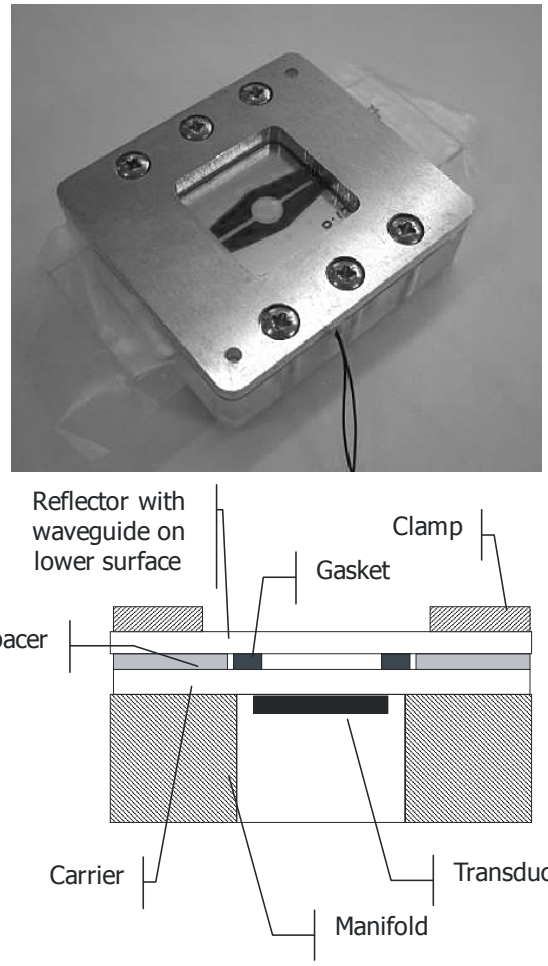

Figure 1: Device acoustic design

Depending on the acoustic contrast factor, acoustic radiation forces tend to drive particles either towards (e.g. polystyrene beads and biological cells in water) or away from (e.g. lipids [14] in water) the pressure nodes of a standing wave. The discussion that follows applies to particles that are driven towards the pressure node.

The device supports three different modes: (a) a near-quarter-wave mode that moves particles toward the reflector, referred to here as the *reflector-quarter-wave* mode, (b) a near-quarter-wave mode that moves particles toward the carrier layer, referred to here as the *carrier-quarter-wave* mode, and (c) a near-half-wave mode.

(a) In the most widely described quarter-wave mode [15, 16], the reflector layer has a thickness of $\lambda/2$ (where λ is the wavelength at the operating frequency) and resonates so that the fluid layer experiences a pressure release boundary condition at the reflector. Combined with a liquid layer of thickness $\lambda/4$, a standing wave is developed such that acoustic radiation forces exert a force towards the pressure node at the fluid/reflector boundary. The disadvantage with this force profile in applications that require particles to be pushed against the reflector (e.g. surface immuno-assays [16]) is that the force tends to zero as the reflector is approached, and a small change in device dimensions (due to manufacturing tolerance) can lead to the node position holding particles close to but not touching the reflector. The device presented here operates in a manner similar to a quarter-wave device, but the actual fluid thickness is 0.74 $\lambda/4$. This is combined with a reflector of thickness 1.027 $\lambda/2$. The resulting acoustic pressure and radiation force profiles (modelled) for this mode (and also the two modes described below) are shown in figure 2. It can be seen that for a particle at the fluid/reflector interface, there is now a positive force into the reflector. An unwanted side effect of this design is that there is a pressure anti-node near the carrier layer, and any particles between this anti-node and the carrier layer will experience a force away from the reflector.

(b) In the *carrier-quarter-wave* mode the thicknesses of the carrier layer and transducer are in resonance (ie their combined thickness is close to $\lambda/2$). This is similar in operation to a reflector-quarter-wave mode except that the resonating reflector has been replaced by the carrier/transducer combination – i.e. a pressure release boundary condition is formed at the fluid/carrier

interface[17]. The result is a force profile that exerts a force towards the fluid/carrier interface on a particle at any position within the fluid layer. Similar to the reflector-quarter-wave case, the fluid thickness in this case is close to but less than λ/4 to ensure that there is a reasonable force at the interface.

(c) The third mode used in the device is a half-wave mode: At its operating frequency, the fluid is in resonance with a pressure node at its centre.

Combining these three modes in a single device, we are able to direct a particle both (a) towards and (b) away from the reflector, and also to hold it (c) centrally in the chamber.

Table 2 lists the experimentally measured and predicted frequencies for the three modes of operation, along with measured amplitudes of the force on a 10μm diameter fluorescent polystyrene bead (Polysciences Inc., Fluoresbrite microspheres). The force measurements were performed by measuring the voltage at which a bead is just levitated, the gravitational force being exactly balanced by the acoustic radiation force [16]. The force data should only be taken as an indication of the order of magnitude of the forces due to the difficulty in establishing exactly when the forces are balanced. The figures correspond to the maximum found within the chamber (near the centre), however observations suggest that there are significant variations across the chamber.

Acoustic Mode	Modelled Frequency (MHz)	Measured Frequency (MHz)	Measured force (pN)
Reflector-Quarter	1.711	1.712	4.1
Carrier-Quarter	1.562	1.508	-
Half	4.649	4.599	2.1

Table 2: Measured and modelled mode frequencies, and acoustic forces. (Force for a 10μm bead at 19Vpp drive voltage)

3 Waveguide and detection of beads

A single-mode waveguide was chosen to illuminate the beads because the optical power distribution in the evanescent field is precisely defined, and the proportion of power in the evanescent field is larger than in a multimode waveguide[1], yielding maximum sensitivity. The laser light source used in all the experiments that follows was a He-Ne laser (Melles Griot) of wavelength 632.8nm.

BK7 glass was chosen as a substrate for the waveguide fabrication. Key factors influencing this choice were having glass that is: sodium rich to enable an ion-exchange waveguide to be produced; low in impurities and bubbles that cause light losses due to scattering; low auto-fluorescence at the working wavelength; and chemically resistant to most biological buffers.

A Potassium ion-exchanged waveguide was produced following the method described by Gortych and Hall [18], with a diffusion time of 60 minutes at 385ºC. This leads to an estimated diffusion depth of 2.3μm and effective waveguide index of 1.52. The propagation loss of the resulting waveguide was measured as 0.16dB/cm.

Light was coupled into the waveguides using prism coupling: a ray of light striking the bottom of the prism is internally reflected, establishing an evanescent field that tunnels across the coupling gap, coupling into the waveguide. To couple into the waveguide a prism was used. To satisfy the phase matching condition (the refractive index of the prism must be higher than that of the periphery of the waveguide) an SF11 prism was used (Edmund Optics NT45-949, n=1.778 at 632.8nm).

For the experiments described below, the chamber was observed with a CCD camera (Basler A202kc) focussed through a 25x microscope objective lens.

As polystyrene beads approach the waveguide surface (in the experiments described in the following section) a wide variation in the intensity – a factor of at least 200 with 10μm beads – of the scattered light is observed. This effect is due to the existence of Whispering Gallery Modes (WGM) [19] or morphology dependent resonances (MDR) in the beads. Simply explained: light is coupled into the surface of the bead, and travels around the bead; if the bead path circumference is an integer number of wavelengths, then the light interferes constructively with itself, and power builds up in the sphere, with photons orbiting the sphere repeatedly, yielding a WGM lifetime depending on the losses. Q-factors of 10^6 are described by Lutti et al. [20] for polystyrene spheres in water. Despite the small variation in microsphere diameters (standard deviations as low as 1.1%), the resulting difference in path lengths are sufficient to cause only a proportion of the beads to resonate. Also, since the beads are not perfectly spherical, the resonance is dependent on the orientation of the bead, and also on whether the bead is adhered to the surface – scattering from a bead rolling along the surface of the waveguide can vary in intensity as it moves in and out of resonance. Exploitation of these whispering-gallery modes has several advantages:

(a) It makes beads scatter light more intensely, so that they can be detected clearly against background scattered light in the waveguide, without the need for fluorescent imaging.

(b) It illuminates a greater proportion of the bead surface. Since the extent of the evanescent field is much smaller than the diameter of the bead, without the WGM only a small proportion of the bead surface is illuminated. When, in the future, the chamber is used for microbead fluorescent assays the WGM light is expected to improve sensitivity dramatically.

The narrow bandwidth of the laser radiation used in these experiments meant that in a small proportion (~10%) of the beads the resonances were not excited strongly enough for the bead to be detected. To ameliorate this effect, broadband excitation will be studied in the future, to allow several resonances to be excited in each bead so that the average intensity of light from each bead is less dependent upon exact size and orientation.

4 Identification of microspheres through flight time measurements

The experiments described here are designed to evaluate the potential of the chamber to assist in the illumination and sensing of fluorophore tagged beads, and in identifying beads based on their size (which will permit multiplexing of several bead types within a single assay).

To identify different sized beads, the beads are timed as they travel between the centre of the fluid chamber (having been positioned there by the half-wave acoustic mode) and the waveguide/reflector under the action of the quarter-wave mode. The acoustic- radiation force, F, on the particle as it travels is proportional to its volume, and hence bead radius, r, cubed. The viscous Stokes drag leads to a terminal velocity,

$$v = \frac{F}{6\pi\eta r} \qquad (1)$$

where η is the effective dynamic viscosity of the fluid [21]. This effective viscosity takes account of the increased drag force experience by the bead as it approaches the wall due to squeeze-film effects. Thus the flight time is proportional to $1/r^2$.

The experimental procedure is as follows: Polystyrene microspheres of diameters 10µm, 20µm (Polysciences Inc., Fluoresbrite microspheres #19096, #18140) and 6µm (Invitrogen PeakFlow Ultra Red, P24671) are diluted with de-ionised water to concentrations of $1.1\text{x}10^6$, $0.2\text{x}10^6$ and $1\text{x}10^6$ beads/ml, respectively, (the lower concentration of 20µm beads ensures that the beads are laterally distinct from one another). The flow chamber is primed by first flushing out bubbles through with a mixture of 50% IPA, 50% water, then flushed with de-ionised water for 1 minute. The beads are introduced by a peristaltic pump, and the flow stopped. The device is oriented with the waveguide vertically below the fluid layer, so beads naturally fall towards the waveguide. To lift the beads, first the carrier-quarter-wave acoustic mode (at 19Vpp transducer voltage) is applied (the half-wave mode has an anti-node in the chamber, and will not lift beads from the waveguide), followed by the half-wave mode (at 19Vpp). This is held for 1 minute to ensure that all the beads are in their equilibrium position, approximately half way between the reflector and carrier layers. The CCD camera (see above) is set to capture at a rate of 30frames/sec. At this point the quarter wave-mode (at 19Vpp) is applied to drive the beads towards the reflector.

The beads are not visible until they reach the evanescent field within a few hundred nanometres of the waveguide surface. By post-processing the captured images, the graphs shown in figure 3 are produced, which show the proportion of beads that have arrived versus time. The data represents the combined data from 15 separate experiments, 5 for each bead size, viewing bead arrivals in an area approximately 1 mm x 1 mm (the field of view of the CCD camera).

The results show that for a particular bead size the arrival times are distributed around a mean arrival time, with sufficiently small standard deviation that the majority of the beads can be identified based on their arrival time at the reflector. Thus, to multiplex between populations of beads simultaneously present in a chamber, a number of images could be acquired over a period of time and the signal from each population determined by suitable post-processing. There are several features of the graphs that need explanation:

The spread in arrival time of the main body of beads: In an ideal case, all the beads of a single size would arrive at once. There are several factors that are non-ideal: (a) the beads vary in diameter (Standard deviations of 1.1%, 3.3%, and 13% for the 6µm, 10µm, and 20µm beads respectively), (b) the strength of the half-wave mode varies across the width of the chamber, (c) the strength of the downward force from the quarter-wave mode varies across the chamber, and (d) Brownian motion of the beads adds a random component to their trajectory.

The 'early' arrivals: Some beads appear to arrive much earlier than would be possible if they had travelled their intended trajectory. We suspect that these beads had not previously left the surface of the reflector, yet were not seen due to a weak WGM resonance. During the experiment, the beads may roll under the action of lateral acoustic radiation forces, and become resonant and hence appear to have 'arrived'. This effect can also cause a bead to fail to be observed when it first arrives, and become visible some time later, also contributing to the spread of arrival times.

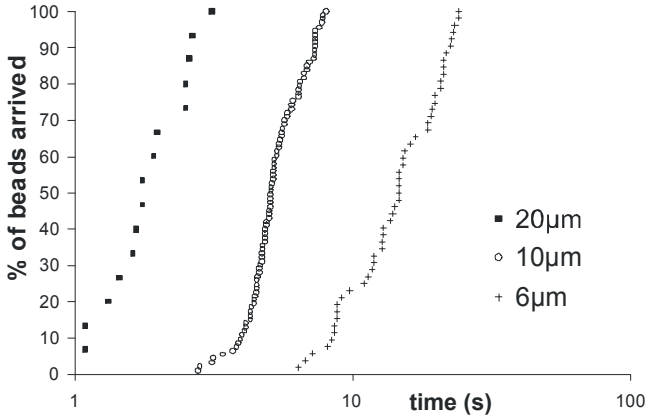

Figure 3: Bead flight times

5 Conclusions

The device presented demonstrates three different acoustic modes useful for manipulating microbeads within a microfluidic chamber. The integrated waveguide permits the illumination of beads in an evanescent field when they are brought to the reflector surface. The beads exhibit whispering gallery mode resonances which enhance the intensity of the illumination, permitting the beads to be observed against the background scattered light. We have shown that beads of different sizes can be differentiated using their flight time between the centre of the cell (held there by the acoustic half-wave mode) and the waveguide surface. In future we plan to unravel the different factors affecting the flight time, and cause the bead arrival times to be more tightly grouped by both reducing lateral variations in acoustic forces through more detailed acoustic design, and also minimising the effect of the WGM on apparent arrival times by using a wide-spectrum illumination source.

Acknowledgements

The authors gratefully acknowledge the support of the EPSRC, DSTL, Point Source, and Genetix.

References

[1] A. D. Wellman and M. J. Sepaniak, "Multiplexed, waveguide approach to magnetically assisted transport evanescent field fluoroassays," *Analytical Chemistry,* vol. 79, pp. 6622-6628, 2007.

[2] N. Jaffrezic-Renault, C. Martelet, Y. Chevolot, and J. P. Cloarec, "Biosensors and bio-bar code assays based on biofunctionalized magnetic microbeads," *Sensors,* vol. 7, pp. 589-614, 2007.

[3] J. W. Chen, M. A. Iannone, M. S. Li, J. D. Taylor, P. Rivers, A. J. Nelsen, K. A. Slentz-Kesler, A. Roses, and M. P. Weiner, "A microsphere-based assay for multiplexed single nucleotide polymorphism analysis using single base chain extension," *Genome Research,* vol. 10, pp. 549-557, 2000.

[4] M. Y. Han, X. H. Gao, J. Z. Su, and S. Nie, "Quantum-dot-tagged microbeads for multiplexed optical coding of biomolecules," *Nature Biotechnology,* vol. 19, pp. 631-635, 2001.

[5] M. Wiklund, J. Toivonen, M. Tirri, P. Hanninen, and H. M. Hertz, "Ultrasonic enrichment of microspheres for ultrasensitive biomedical analysis in confocal laser-scanning fluorescence detection," *Journal Of Applied Physics,* vol. 96, pp. 1242-1248, 2004.

[6] T. Lilliehorn, U. Simu, M. Nilsson, M. Almqvist, T. Stepinski, T. Laurell, J. Nilsson, and S. Johansson, "Trapping of microparticles in the near field of an ultrasonic transducer," *Ultrasonics,* vol. 43, pp. 293-303, 2005.

[7] Y. Abe, M. Kawaji, and T. Watanabe, "Study on the bubble motion control by ultrasonic wave," *Experimental Thermal and Fluid Science,* vol. 26, pp. 817-826, 2002.

[8] A. Neild, S. Oberti, F. Beyeler, J. Dual, and B. J. Nelson, "A micro-particle positioning technique combining an ultrasonic manipulator and a microgripper," *Journal of Micromechanics And Microengineering,* vol. 16, pp. 1562-1570, 2006.

[9] M. Gröschl, "Ultrasonic separation of suspended particles - Part I: Fundamentals," *Acustica,* vol. 84, pp. 432-447, 1998.

[10] J. J. Hawkes and W. T. Coakley, "Force field particle filter, combining ultrasound standing waves and laminar flow," *Sensors and Actuators B-Chemical,* vol. 75, pp. 213-222, 2001.

[11] M. Hill, Y. Shen, and J. J. Hawkes, "Modelling of layered resonators for ultrasonic separation.," *Ultrasonics,* vol. 40, pp. 385-92, 2002.

[12] G. L. Duveneck, A. P. Abel, M. A. Bopp, G. M. Kresbach, and M. Ehrat, "Planar waveguides for ultra-high sensitivity of the analysis of nucleic acids," *Analytica Chimica Acta,* vol. 469, pp. 49-61, 2002.

[13] Krimholt.R, D. A. Leedom, and G. L. Matthaei, "New Equivalent Circuits for Elementary Piezoelectric Transducers," *Electronics Letters,* vol. 6, p. 398, 1970.

[14] F. Petersson, A. Nilsson, C. Holm, H. Jonsson, and T. Laurell, "Continuous separation of lipid particles from erythrocytes by means of laminar flow and acoustic standing wave forces," *Lab on a Chip,* vol. 5, pp. 20-22, 2005.

[15] M. Hill, "The selection of layer thicknesses to control acoustic radiation force profiles in layered resonators," *Journal of the Acoustical Society of America,* vol. 114, pp. 2654-2661, 2003.

[16] S. P. Martin, R. J. Townsend, L. A. Kuznetsova, K. A. J. Borthwick, M. Hill, M. B. McDonnell, and W. T. Coakley, "Spore and micro-particle capture on an immunosensor surface in an ultrasound standing wave system," *Biosensors and Bioelectronics,* vol. 21, pp. 758-767, 2005.

[17] N. R. Harris, M. Hill, Y. Shen, R. J. Townsend, S. P. Beeby, and N. M. White, "A dual frequency, ultrasonic, microengineered particle manipulator," *Ultrasonics,* vol. 42, pp. 139-44, 2004.

[18] J. E. Gortych and D. G. Hall, "Fabrication of Planar Optical Wave-Guides by K+-Ion Exchange in BK7 and Pyrex Glass," *IEEE Journal of Quantum Electronics,* vol. 22, pp. 892-895, 1986.

[19] F. Vollmer, D. Braun, A. Libchaber, M. Khoshsima, I. Teraoka, and S. Arnold, "Protein detection by optical shift of a resonant microcavity," *Applied Physics Letters,* vol. 80, pp. 4057-4059, 2002.

[20] J. Lutti, W. Langbein, and P. Borri, "High Q optical resonances of polystyrene microspheres in water controlled by optical tweezers," *Applied Physics Letters,* vol. 91, 2007.

[21] P. H. Brenner, "The slow motion of a sphere through a viscous fluid towards a plane surface," *Chemical Engineering Science,* vol. 16, pp. 242–251, 1961.